A NEW THREE-DIMENSIONAL THERMOSPHERIC MODEL BASED ON SATELLITE DRAG DATA

F. Barlier*, C. Berger*, J.L. Falin*, G. Kockarts and G. Thuillier*****

**CERGA, F - 06130 Grasse, France*
***IAS, B - 1180 Bruxelles, Belgique*
****Service d'Aéronomie, F - 91370 Verrières le Buisson, France*

ABSTRACT

Using satellite drag data a three-dimensional thermospheric model is developed in terms of spherical harmonics. The model gives total density, partial densities (He, O, N_2) and thermopause temperature as a function of solar and geomagnetic activity, local time, day of the year, altitude and latitude.

INTRODUCTION

A sufficiently large amount of total density values deduced from satellite drag data allow a spherical harmonic analysis when a type of vertical distribution is adopted for the temperature and the partial densities. We used 36000 total densities spread over almost two solar cycles with an excellent geographical coverage.

METHOD

The 36000 total densities ρ are selected from an initial data file of 70000 values [1] in a way such that each density obeys one of the following criteria : $\rho(He) > 0.7\ \rho$ or $\rho(O) > 0.7\ \rho$ or $\rho(N_2) > 0.5\ \rho$ in the height range 200 - 1200 km. Each partial density is distributed vertically according to the relation

$$\rho_i(z) = A_{i1} \exp [\ G_i(L) - 1\ ]\ f_i\ (z) \qquad (1)$$

where $f_i(z)$ is the vertical diffusive equilibrium distribution when the partial density at 120 km altitude is equal to one. $G_i(L)$ is a spherical harmonic expansion [2] which depends on 35 unknown coefficients. The thermopause temperature involved in (1) is given by

TABLE 1. Coefficients A_j (j = 1,36)

j	T_∞	He	O	N_2
1	9.9980 E + 02	3.0016 E + 06	1.0320 E + 11	3.8420 E + 11
2	- 3.6357 E - 03	1.6926 E - 01	- 1.6598 E - 03	2.8076 E - 02
3	2.4593 E - 02	- 6.2624 E - 02	- 9.9095 E - 02	4.8462 E - 02
4	1.3259 E - 03	2.3799 E - 03	7.8453 E - 04	- 8.1017 E - 04
5	- 5.6234 E - 06	- 3.1008 E - 05	- 2.3733 E - 05	2.0983 E - 05
6	2.5361 E - 03	5.6980 E - 03	8.0001 E - 01	2.9998 E - 03
7	1.7656 E - 02	1.7103 E - 02	- 1.0507 E - 02	1.8545 E - 02
8	3.3677 E - 02	- 1.7997 E - 01	- 1.6311 E - 01	3.4514 E - 02
9	- 3.7643 E - 03	- 1.3251 E - 01	1.4597 E - 01	5.3709 E - 02
10	1.7452 E - 02	- 6.4239 E - 02	1.0517 E - 01	- 1.3732 E - 01
11	- 2.1150 E + 02	2.2136 E + 02	3.7357 E + 00	8.6434 E + 01
12	- 2.7270 E - 03	2.4859 E - 01	2.4620 E - 01	1.9930 E - 02
13	2.7465 E - 02	- 1.7732 E - 01	- 5.0845 E - 02	- 8.4711 E - 02
14	- 9.5216 E + 01	1.0541 E + 02	1.0775 E + 02	8.9339 E + 01
15	- 1.3373 E - 01	- 1.1071 E + 00	3.9103 E - 01	- 4.9083 E - 02
16	- 2.7321 E - 02	- 3.6255 E - 02	9.6719 E - 02	9.1420 E - 03
17	- 9.6732 E - 03	- 1.0180 E - 01	1.2624 E - 01	- 1.6362 E - 02
18	- 1.4584 E + 01	- 1.9548 E + 02	- 1.6608 E + 01	4.9234 E + 01
19	- 2.7469 E - 02	1.1711 E - 01	- 1.4463 E - 01	- 4.6712 E - 02
20	- 1.7398 E + 02	- 2.1532 E + 02	1.0964 E + 02	5.2774 E + 01
21	- 6.6567 E - 02	- 3.1594 E - 01	- 2.0686 E - 01	—
22	- 5.9604 E - 03	5.2452 E - 02	8.2922 E - 03	—
23	6.7446 E - 03	- 3.1686 E - 02	- 3.0261 E - 02	—
24	- 2.6620 E - 02	- 1.3975 E - 01	1.4237 E - 01	—
25	1.4691 E - 02	8.3399 E - 02	- 2.8977 E - 02	—
26	- 1.0971 E - 01	2.1382 E - 01	2.2409 E - 01	—
27	8.8700 E - 03	- 6.1816 E - 02	- 7.9313 E - 02	—
28	3.6918 E - 03	- 1.5026 E - 02	- 1.6385 E - 02	—
29	1.2219 E - 02	1.0574 E - 01	- 1.0113 E - 01	—
30	- 7.6358 E - 03	- 9.7446 E - 02	6.5531 E - 02	—
31	- 4.4894 E - 03	2.2606 E - 02	5.3655 E - 02	—
32	2.3646 E - 03	1.2125 E - 02	- 2.3722 E - 03	—
33	5.0569 E - 03	- 2.2391 E - 02	1.8910 E - 02	—
34	1.0792 E - 03	- 2.4648 E - 03	- 2.6522 E - 03	—
35	- 7.1610 E - 04	3.2432 E - 03	8.3050 E - 03	—
36	9.6385 E - 04	- 5.7766 E - 03	- 3.8860 E - 03	—

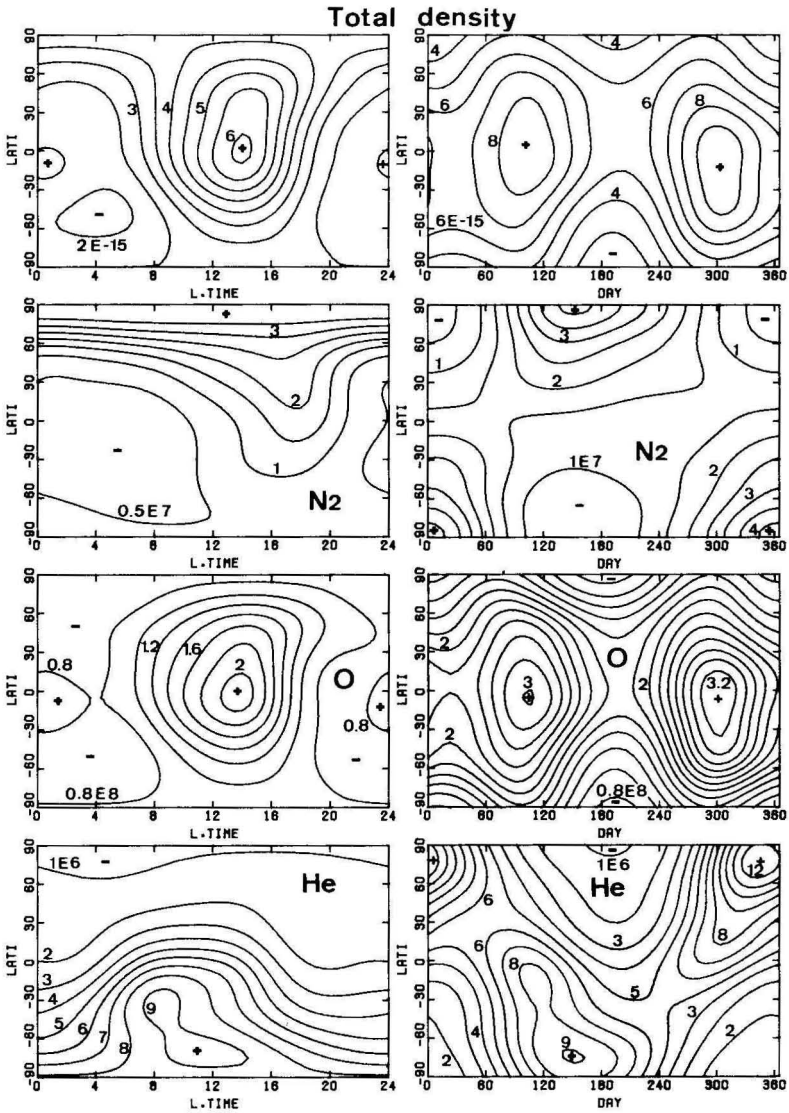

Fig. 1.- Local-time latitude maps (left part) and day of the year-latitude maps (right part) for June solstice at 400 km with a mean solar decimetric flux $F = \bar{F} = 150 \times 10^{-22}$ W m^{-2} Hz^{-1} and $K_p = 2$. Total density contours are given in g cm^{-3} (top panels) and concentrations are given in cm^{-3} (lower six panels).

$$T_\infty = A_1 G(L) \qquad (2)$$

The 36 coefficients for T_∞ are given [3] in TABLE 1. A least squares fitting of equation (1) leads to the coefficients A_j (j = 1,36) given in TABLE 1 for He, O and N_2. The form of $G_i(L)$ is identical to that one presented in [3] with the exception that for helium the factor (1 + F1) is omitted in the diurnal, semi-diurnal and terdiurnal terms as well as in the annual and semiannual terms. A full account of the computational technique is presented elsewhere [1] . Molecular oxygen concentration is kept constant to a value of 4.75 x 10^{10} cm^{-3} at 120 km where the temperature is 380 K. The vertical temperature profile [4] is computed with T_∞ from (2) and a slope parameter s = 0.02.

RESULTS

Figure 1 gives an example of the results obtained with this model at 400 km. Diurnal variations of ρ , $n(N_2)$, n(O) and n(He) are seen on the left part of the figure, whereas annual variations are presented on the right part. The usual characteristics of the thermospheric structure are apparent. It should be emphasized that the partial concentrations are deduced from the total density data and that they generally agree with in situ determinations.

The maximum of the total density on 21 June does not appear near the subsolar point but it is located near the geographic equator. This feature is a consequence of the behavior of atomic oxygen which is the major constituent at 400 km altitude. The slow decrease of ρ towards the north pole is explained by the temperature increase in this region. It is also to be noted that the individual constituents have their diurnal maximum at different local times. Finally the winter helium bulge is clearly seen on the right part on Fig. 1 and the seasonal variation is larger at the northern pole than at the southern pole.

REFERENCES

1. F. Barlier et al., Annls. Géophys. to be published, 34, (1978).
2. A.E. Hedin et al., J. Geophys. Res. 79, 215 (1974).
3. G. Thuillier et al., J. Atmos. Terr. Phys. 39, (1977).
4. J.C.G. Walker, J. Atmos. Sci. 22, 462 (1965).